

# Electric Lift Augmentation of Scientific Balloons Using Gossamer Blades

Nicholas Kenny<sup>a</sup> and Dale Lawrence<sup>a</sup>

Currently, the HYFLITS campaign collects turbulence and particulate measurements between approximately 20 and 34 km using 1500-3000 g latex balloons. The balloons employ a venting system which allows controlled descents through the measurement altitudes. This descent period is critical, as turbulence data cannot be taken on ascent due to the wake of the balloon itself. Particulate measurements may also be corrupted by small particles shedding off the balloon. A control system which would allow for multiple altitude profiles would greatly increase the amount of usable data from each flight by increasing the number of descents through the measurement region.

While this venting technique enables a single descent, it cannot be used to perform multiple altitude profiles. Unlike large scientific balloons, there has historically been a lack of control solutions for small, inexpensive, long duration balloons operating at high altitudes. Electric lift augmentation, which uses centripetal forces to spin up gossamer propeller blades, aims to address this by creating a small amount of lift with or against natural buoyancy.

Numerous tests of this lift augmentation concept have been conducted to help determine the feasibility of the system. Results from the latest tests demonstrating blade angle stability are presented. In addition to physical testing, an analytical model utilizing blade element theory addresses conceptual questions relating to the scalability of an electric lift augmentation system on a balloon. Power consumption on the order of 5-20 W appears achievable for ascent/descent rates of 1-2 m/s. This would enable indefinite operation with high performance commercial solar panels and batteries sized only for overnight operation. With more than just profiling applications, the lift augmentation device would enable altitude targeting, rudimentary station keeping, and long duration controlled flights in the atmospheres of other planets.

Balloon control | Feasibility | Mission applications | Stability

---

## Acknowledgments

Funding for this work comes from the Air Force Office of Scientific Research (AFOSR) grant FA9550-18-1-0009.

---

<sup>a</sup> Aerospace Engineering Sciences, University of Colorado Boulder  
E-mail: nicholas.kenny@colorado.edu

## 1. Introduction to Balloon Altitude Control

Fundamentally, balloons operate on a balance between balloon free lift, Eq. 1 and drag, Eq. 2.

$$F_L = V(\rho_{air} - \rho_{gas})g - (m_p + m_b)g \quad [1]$$

$$F_D = \frac{1}{2}C_D A \rho_{air} w^2 \quad [2]$$

Here,  $V$  is the volume of the balloon envelope,  $\rho_{air}$  is the air density,  $\rho_{gas}$  is the density of the lifting gas,  $g$  is the acceleration due to gravity, and  $m_p$  and  $m_b$ , and are the masses of the payload and balloon itself.  $C_D$  is the drag coefficient of a spherical balloon,  $A$  is the sphere's cross sectional area, and  $w$  is relative wind velocity as seen by the balloon. By setting  $F_L$  and  $F_D$  equal, and assuming the balloon rises in still air, the ascent rate is then

$$w_a = \sqrt{\frac{2F_L}{C_D A \rho}} \quad [3]$$

Control options are limited, as the drag coefficient, balloon area, and payload mass are typically fixed. Additionally, the air density is also fixed, following a known profile as the balloon translates through the atmosphere. This leaves just changes in the lifting gas, balloon mass, and balloon volume available for augmenting the natural dynamics of the balloon system.

A summary of methods to provide balloon altitude control is shown in Table 1.

Venting is already being utilized on HYFLITS launches to enable a controlled descent from apogee through the measurement region of interest (2). In conjunction with additional payload ballast, balloons can also be made to ascend (1). Venting and ballast techniques offer one of the simplest, most lightweight solutions to balloon altitude control, but suffer from a major scalability problem. Control is inherently limited by how much lifting gas can be vented and how much ballast you can bring to drop. Additionally, when using latex balloons, the apogee is limited to a critical strain where the balloon loses elasticity and can no longer expel lifting gas on its own (2). This may also limit subsequent ascents/descents when ballast is used, as the balloon may not be elastic enough to expel helium again at apogee. The double balloon method is similar to venting except that an entirely contained pocket of gas is released all at once (3), along with the balloon mass that contained it.

Air ballast is a popular control technique because of its relative simplicity, particularly on larger balloons. Requiring only an additional internal bladder inside an existing balloon and a pump to move this air in and out, air ballast systems have a low mass impact compared to other techniques and offer the possibility of operating indefinitely. As the ballast air only

**Table 1. Summary of Altitude Control techniques for balloons.**

Control Method	Referenced	Summary
Venting and Ballast	(1), (2)	A zero pressure balloon is fitted with a vent valve and may carry additional ballast mass. When the vent is opened, lifting gas is released and the balloon descends. If ballast is released, the payload mass decreases and the balloon ascends.
Double Balloon	(3)	Two balloons are used on ascent. At apogee, one balloon is cut away and released. This results in a more controlled descent under the remaining "balloon parachute."
Mechanical Compression	(4), (5)	A superpressure balloon is "pinched" to reduce its overall volume while the amount of gas remains the same. This results in a change in buoyancy, leading to ascents or descents.
Air Ballast	(4)	Ballast gas is pumped in to or out of a bladder inside a superpressure balloon, changing the density of the superpressure balloon to ascend or descend.
Differential Expansion	(4), (6), (7)	Air from a zero pressure balloon is pumped into or out of a superpressure envelope, resulting in a volume reduction of the zero pressure balloon and a change in buoyancy. Opposite of air ballast.
Phase Changing Fluid	(8), (9)	Similar to differential expansion but uses a liquid fluid which undergoes a phase change to a gas as internal or atmospheric temperatures rise and fall, resulting in a volume change of the balloon and changes in buoyancy.
Lifting Orbiter	(10)	Uses a powered, tethered wing "orbiter" that generates lift against the balloon's buoyancy, allowing for changes in altitude from a neutrally buoyant level.

needs to be heavier than the lifting gas, often ambient air is used. A primary disadvantage however is that as the air density decreases with the ascending balloon, it becomes much harder to effectively pump. This limits the operational altitude of air ballast systems to under approximately 5km (4). Another issue which limits its effective apogee is that of freezing air. Without conditioning the air being pumped, moisture in the air can freeze within the bladder, possibly causing ruptures (4).

Differential expansion is functionally the opposite of air ballast. Instead of pumping external air into a flexible bladder, lifting gas is pumped from a flexible, zero pressure balloon into a rigid superpressure bladder. Differential expansion exhibits many of the same benefits of air ballast systems in that it remains relatively simple and lightweight. It also suffers similar drawbacks in the difficulty of pumping low-density air, but not from the freezing issue (as the superpressure bladder can be made more tolerant to temperature fluctuations) (4). Still, differential expansion is theorized to be effective only up to approximately 20 km (4), (7). A final drawback of both air ballast and differential expansion is that due to the time required to pump, they are not effective at controlling balloons over short-durations, instead suited more for maintaining a specific altitude over diurnal cycles, as demonstrated in (6).

All of these methods take advantage of transporting air around the system in some way, often quite difficult to do at high altitudes and for a small amount of power. A solution which can operate on electricity is desired because this could allow a balloon to potentially operate indefinitely, using solar panels to power the control system. The balloon would also be operating above the clouds, so batteries would only need to be sized to operate through the night rather than having to account for unpredictable atmospheric obstructions. This

would necessitate a low power consumption control scheme however, as solar panels could quickly start to contribute to a significant fraction of overall payload mass, reducing the available mass for scientific payloads.

Mechanical compression is one method that could operate electrically and doesn't require air transport from one reservoir to another. By pinching or compressing the outer balloon envelope, the balloon's volume decreases (with a corresponding increase in internal pressure). From Eq. 1, this results in a smaller balloon lift thereby causing a reduction in float altitude until the ambient air density increases to compensate (4). This may also correspond to a change in balloon drag, the direction and magnitude of this change would be dependent on how the balloon was compressed (5). The force required to compress the balloon tends to zero as the superpressure difference decreases, so control could be accomplished with extremely lightweight and low power actuators (4). However, the altitude range that can be achieved depends on how much the balloon can be compressed, and without complicated structures and multiple compression actuators, volume change is only on the order of approximately 50%, resulting in only a handful of kms of control authority (5). It also requires the use of superpressure balloons, which are more expensive and not being used by the HYFLITS team.

Another method utilizes a phase-changing fluid, which is a liquid at one temperature and pressure in the flight regime and a gas at another. This concept was tested at JPL in 1994 in a test campaign called the Balloon **AL**titude **C**ontrol **E**xperiment (ALICE) (8). In the tests, refrigerant R114 was used, which transitions from a gas at sea level to a liquid above approximately 4-7 km. While this would not be very applicable to the HYFLITS team, the original ALICE testing was to validate the same concept for use on Venus. Similar concepts have been proposed using water as a lifting gas on Venus, which would target different altitudes (9). While the concept is simple and lightweight, its sensitivity to specific atmospheric conditions makes it unsuitable for general balloon control.

The final method discussed is a design explored by a Senior Projects Team at CU Boulder called a High Altitude Lifting Orbiter (HALO)(10). HALO uses a small wing on a 5 m tether to augment the lift of the balloon, powering the orbiting wing with a small propeller. The wing, made of lightweight foam and designed with similar constraints in mind to the HYFLITS team, weighs less than 1.5 kg. Further iteration on this concept could improve performance. This idea is fundamentally different from the others presented in that rather than modifying an existing variable in the free lift equation, it introduces an entirely new "augmented lift" term, in this case, aerodynamic lift.

While the HALO concept does suggest the possibility of providing sustained balloon control electrically, the relatively small propeller (0.45 m) coupled with the extremely thin air at the altitudes HYFLITS operates results in low power efficiency. We can see this effect in practice on the Mars Ingenuity Helicopter, which utilizes larger 1.2 m propellers to fly in the thin atmosphere of Mars. While the system weighs only 1.8 kg, it requires up to 500 W of power and can only operate for 90-180 seconds before having to land and recharge its batteries (11). Instead, inspiration can be taken from heliogyros (12), a type of solar sail, in order to extend the HALO concept from a small propeller powering a small wing to an extremely large propeller which is in itself gossamer, deriving its structure and rigidity from strings

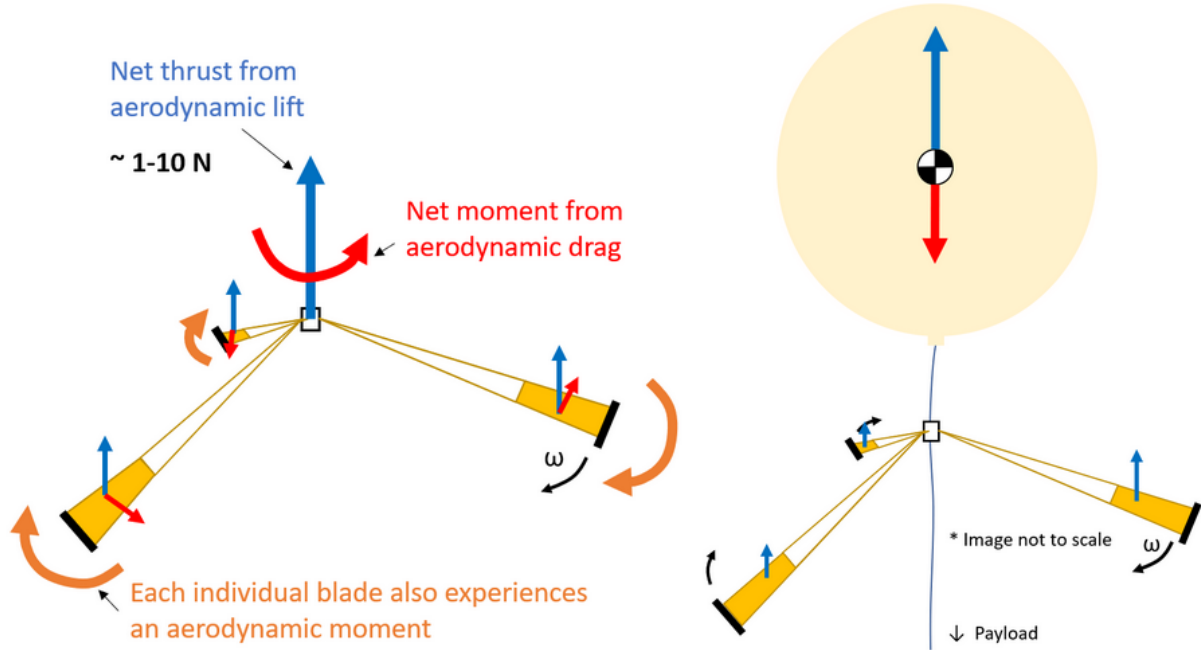


**Fig. 1.** Left: Forces and moments acting on a flexible, gossamer blade generating aerodynamic lift to augment the natural buoyancy of the balloon. Right: Lift augmentation device on a small weather balloon, with the net free lift shown larger than drag due to the thrust of the blades.

tensioned through centripetal forces. Figures (1) and (2) describe such a concept. While appearing and functioning like a helicopter propeller, this gossamer blade lift augmentation strategy does not need to provide enough lift to “fly” like a helicopter does. Instead, it only needs to produce on the order of 1-10 N of thrust in order to upset the balance of the free lift vs balloon drag equation, resulting in an ascent or descent speed of 1-2 m/s. Because of drag, the blades will always lag behind a perfectly radial outward-pointing direction when spinning (angle  $\beta$  in the top view of Fig. (2)), called the lag angle. Additionally, unless the lift force is greater than that of gravity, the blade will always hang below a perfectly perpendicular direction, called the coning angle (angle  $\theta$  in the side view of Fig. (2)). Variations around a nominal coning angle are often referred to as blade flap, whereas variations around a nominal lag angle are simply oscillations in the lag angle. A major difference in heliogyros compared to this concept is the source of the thrust. As a type of solar sail, heliogyros derive thrust from solar radiation pressure. Such pressure does not produce a moment on the blades, which is produced in the generation of the aerodynamic lift that provides thrust to the balloon system.

## 2. Current Progress

Four prototypes, each addressing lessons learned from the previous version, have been built and tested since April 2021. Utilizing a commercial ceiling fan to spin the rotor, the goal of these tests was to quickly assess the feasibility of the concept. Figure (3) shows the Ver.

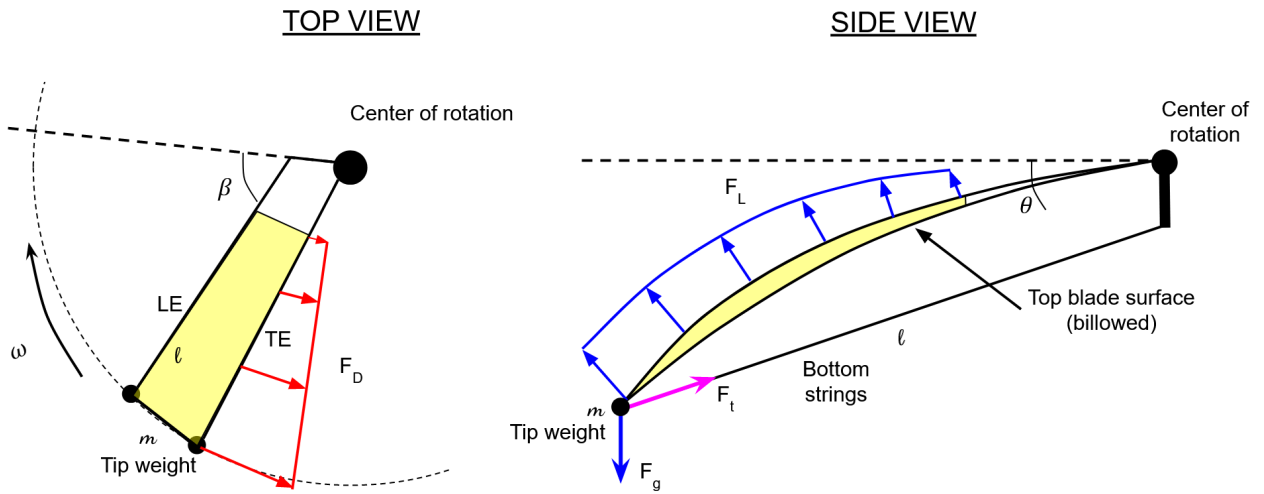


Fig. 2. Left: Top view of a single blade showing how aerodynamic drag contributes to the lag angle  $\beta$ . Right: Side view of a single blade showing the billowed shape the flexible blades take due to the lift they generate. This also affects the coning angle  $\theta$ .

4 model in the ASPEN testing lab on the CU Boulder campus. While previous versions demonstrated static blade angle of attack stability using active controllers, they suffered from a number of drawbacks that necessitated a redesign in order to continue testing effectively. In particular, three main areas were addressed:

1. A need for increased angular resolution of the string deployment servos, and the ability to store a longer length of string during the deployment process. This would allow for more precise control of string length and blade angle of attack while allowing test conductors to spin up the device to greater speed without tangling.
2. A requirement for real-time string length adjustment during a test (rather than needing to stop the fan to adjust strings by hand). In addition to enabling the possibility of trimming each blade's angle of attack, this would also allow for prescribed angles of attack to be reached.
3. Previous tests were evaluated qualitatively using video recordings, making true comparisons between subsequent tests difficult. Instead, quantitative data needed to be collected and processed so that more specific conclusions could be drawn about blade performance.

Design modifications would also need to positively impact the scalability of the system. For example, while the Vicon system in the ASPEN lab could be used to collect data on the blades, such a system would not be viable for larger prototypes (that might be tested outside) or on a full scale lift augmented balloon. It would also require significant development towards new data processing and analysis codes. One major change was geometric and resulted in a method of rigging the strings in a way which would provide natural static stability by taking advantage of a 4-bar link. This new rigging, compared to previous versions, can be seen in Fig. (4).



**Fig. 3.** Full V4 prototype hanging in the ASPEN Lab ready for testing. Note the blade tips, which were used for previous versions, are inactive and only used as tip weight. Overall, the device weighs approximately 1.7 kg in its current configuration.

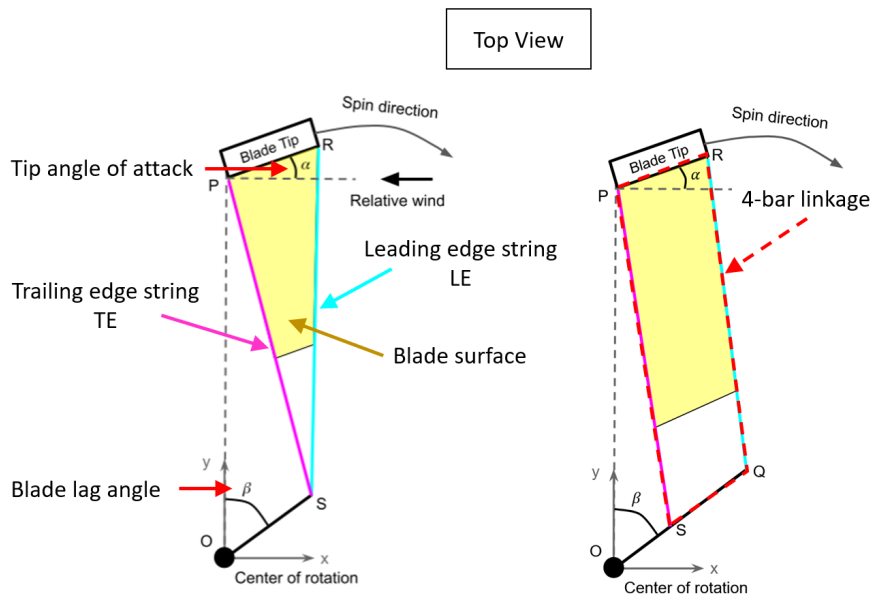


**Fig. 4.** Comparison of the previous rigging method (left) with the new rigging method which takes advantage of a 4-bar linkage (right). Note that two parallel "bars" are flexible and made of string.

In order to get better resolution from the servos, a gear reduction system was designed. This was advantageous over purchasing new, higher quality servos since a full scale lift augmentation device is not necessarily intended to be recovered. Modification of the servos was necessary to enable continuous rotation, and flight software had to be rewritten to account for this. Further, as the final 10:1 gear reduction required significantly more space than was available on the blade tips, the entire line length control system was relocated to the gondola. Doing so also enabled a reduction in overall system complexity from an electronics point of view, as now a single microcontroller could monitor and manage all three blades rather than 3 separate microcontrollers each monitoring their own blade. Additionally, these larger spools enabled a 10x increase in stored string, allowing the device to deploy blades up to 5 m long. The new spools can be seen in Fig. (5).

While the previous line deployment mechanism was controlled remotely with a hobby RC controller, coordination of all 6 servos manually would be difficult. Instead, a remote ground station which could communicate to the lift augmentation gondola was designed and consisted of a low power radio module (who's pair was on the gondola), an Arduino for interfacing with the radio, and a MATLAB GUI for ease of use. Figure. (6) shows a schematic of this as well as the GUI's layout. An operator could select which blade (or groups of blades) needed adjustment, then could individually control differential and collective inputs to that blade (or group). This enabled real-time commanding of the blade angle as well as the ability to trim the blades individually without needing to stop the device. This also allowed for telemetered data from the gondola that could be analyzed after tests.

That telemetered data consisted of blade positions in 2D space measured by optical tracking cameras mounted to the gondola itself. Three OpenMV Cam H7's were mounted

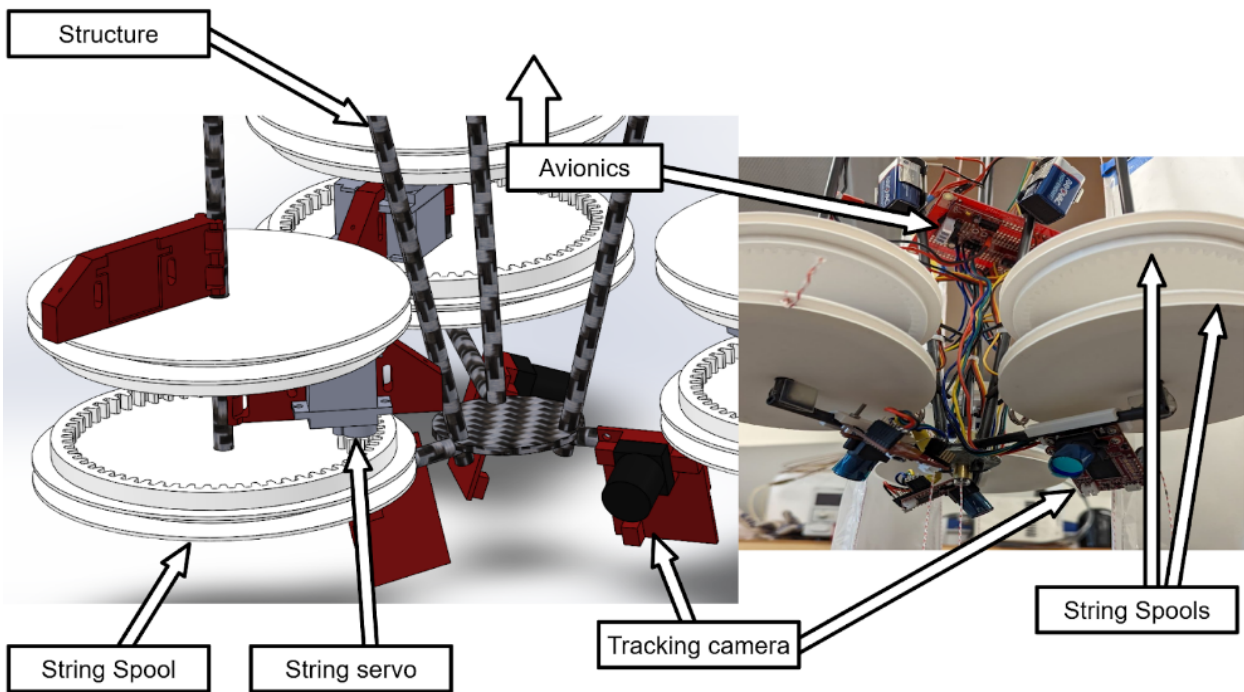


Fig. 5

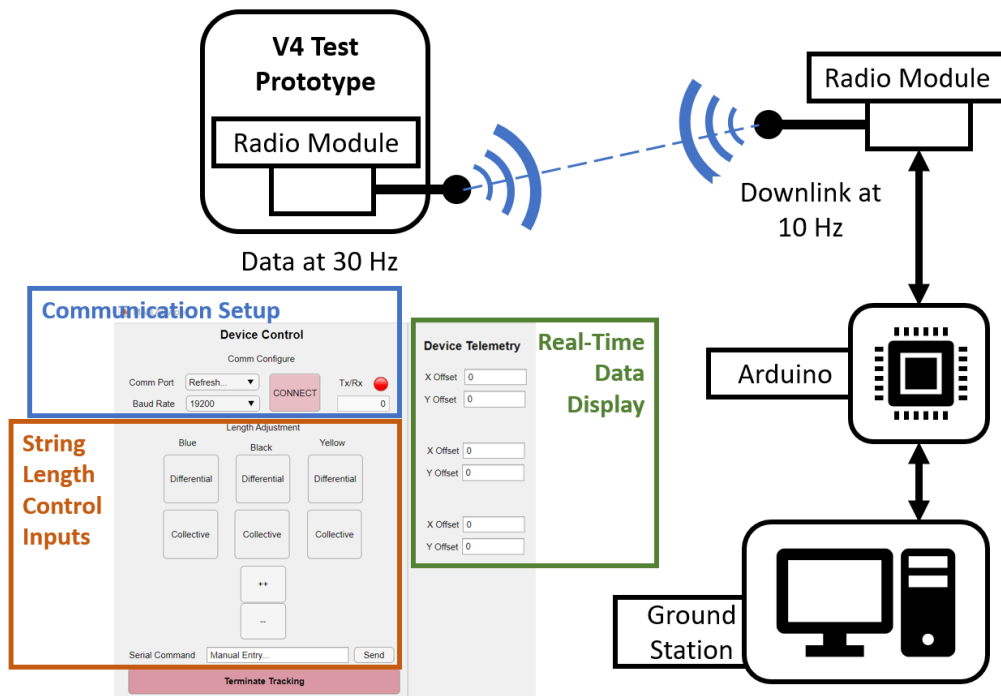


Fig. 6. CAD view (left) and final detailed view (right) of the lower portion of the V4 lift augmentation device, which includes more of the mounting for string length control components, avionics, and sensors.

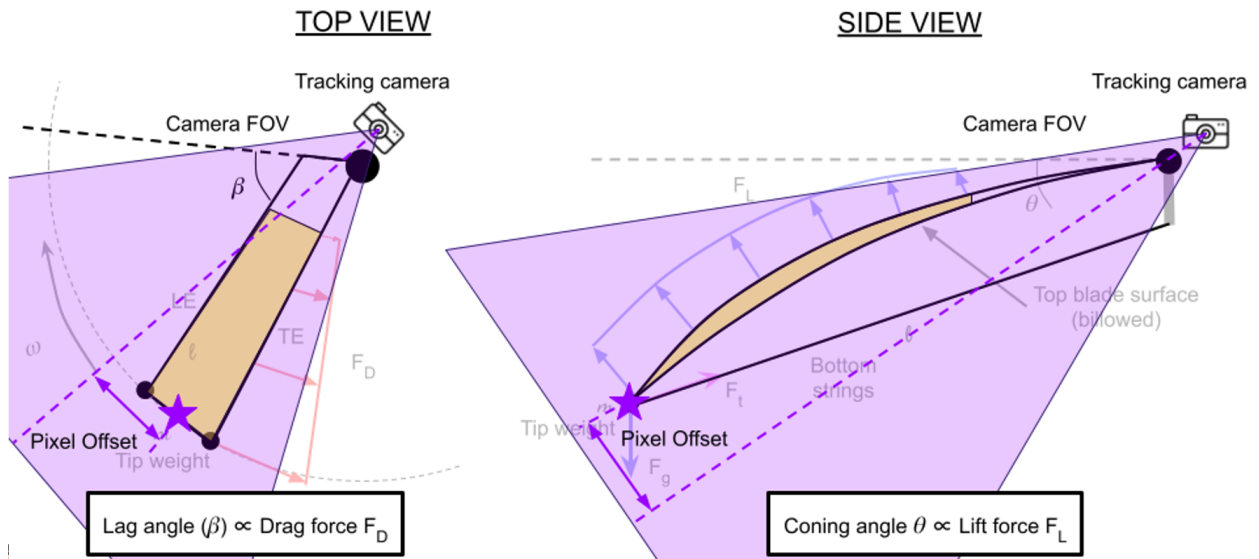
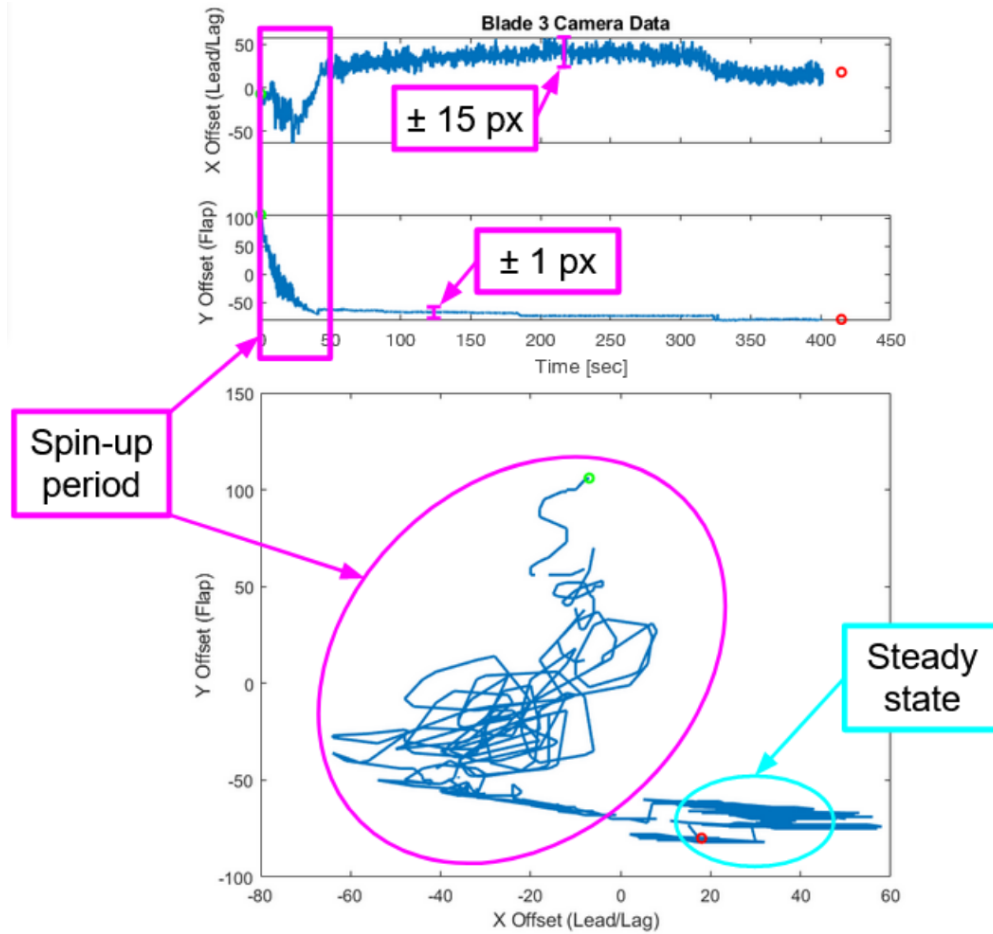


Fig. 7. Top and side views from Fig. 2 with the approximate camera field of view overlaid demonstrating how the cameras are used to measure the lag angle and coning angle of the device while testing.

with their field of view pointing down and out towards the blade tips as seen in Fig. (7), now fitted with a 635 nm red LED. The cameras were also fitted with an inexpensive bandpass filter (bandwidth: 110 nm, center: 659 nm). In conjunction with software filtering that was implemented on-camera, the position of the tracking LED could be determined within the frame using a blob detection algorithm. This pixel location was sent to the gondola microcontroller for forwarding to the ground station.

The results of these improvements represented a huge milestone in the development of the lift augmentation device. Figure (8) shows the data from one test of a single blade.

In the plots, the unsteady spin-up period is clear for the first approximately 50 seconds of the test. Once the blades settle, their flap is nearly non-existent, with the blade tips only flapping a single pixel up and down. In its current configuration, one pixel corresponds to approximately 1.2 cm of translation, meaning the tip only oscillates up and down (flap) around a couple of centimeters. The blades oscillate around a nominal lag angle by approximately 15 pixels, or 18cm. Also clearly visible are changes in the blade coning angle as changes to the fan spin speed are prescribed. These can be seen at approximately 180 sec and 325 sec into the test in Fig. (8). A critical step in the development and testing process, this was the first time the blades could really be considered naturally stable, with previous tests often resulting in blade flap on the order of 30 cm or more and lag angles sometimes exceeding  $90^\circ$ , resulting in tangling. These results enable future exploration and optimization, as the fundamental problem of blade stability appears surmountable using this 4-bar linkage rigging method that is not necessary when applying similar concepts to heliogyros due to the lack of aerodynamic effects. Future work will include a more precise mounting method for the cameras so that the correlation between pixel offset or tip translation distance and absolute coning and lag angles can be derived.



**Fig. 8.** Data from one of the tracking cameras demonstrating the unsteady spin-up period and subsequent stable operation of a blade of the lift augmentation device. 1 pixel represents approximately 1.2cm of translation at the tip.

### 3. Future Scalability

Concurrently to physical testing, an analytical model designed to explore the scalability of the lift augmentation device was being developed. Intentionally decoupled from blade dynamics and specific rigging configurations, the scalability model is designed to answer questions like, "Given a prescribed lift:drag ratio, how fast would a lift augmentation device need to spin in order to cause an ascent/descent rate of X m/s?" and "If the blades spun at Y rpm, how fast would the balloon need to spin in order to counter the torque with viscous drag effects across the balloon surface?"

The model implements the balloon ascent model from (13) but adds an aerodynamic lift term. This aerodynamic lift, which comes from the blades, is calculated using blade element theory. To calculate the drag of the balloon, Boyle's Law is used to calculate the volume (and subsequently the frontal area) of the balloon at varying altitudes which then directly feed into Eq. 2.

The current model assumes 3 blades each 3 m in length with membrane covering the outer 20% of the device. It also assumes a balloon which is between 6 and 12 m in diameter depending on the altitude between 20 and 35 km. It predicts that, for a desired 2 m/s translation rate in altitude and a blade coning angle of  $45^\circ$ , the blade rotation rate is between 90 rpm at 20 km up to 185 rpm at 35 km. This results in a balloon rotation rate of nearly 2000 rpm at 20 km and only 60 rpm at 35 km, applying assumptions for viscous drag on a sphere from (14). While initially unintuitive, this makes sense since even though the air is thinner at 35 km (which would suggest a decrease in viscous balloon drag for a fixed rotation rate compared to lower altitudes). The thin air also means less drag from the blades and therefore less required reaction torque to counter their rotation. Further, the balloon surface area is greatly increased at higher altitudes due to the reduced ambient pressure, so viscous drag effects on the balloon surface are increased. The torque and RPM requirements are summarized in Fig. 9. It is unlikely that the balloon could actually spin at 2,000 rpm without rupturing, however the balloon spin rates decrease exponentially with altitude. If only a 1 m/s translation is required, the balloon spins less than 152 rpm above 25 km, which is much more reasonable. The fidelity of the model for balloon spin rate is something that will be increased in the future, as it is still unclear how applicable the assumptions of a spherical balloon and viscous torque apply at these low Reynolds numbers.

The model also addressed power and energy consumption, with results shown in Fig. 10. It was determined that in order to translate from 20 km to 35 km at 2 m/s, cumulative energy consumption would be slightly over 25 Whrs, with the maximum instantaneous power consumption being under 20 W. This is easily achievable by high-performance commercial solar cells. While not fitting all design requirements (namely, being too large and producing too low of an individual cell voltage), Maxeon Gen II cells\* offer a power density of nearly  $220 \text{ W/m}^2$ , meaning that continuous operation would only require  $0.1 \text{ m}^2$  of solar area. Such a panel array would only weigh approximately 58 g, as each cell weighs only 6.5 g.

---

\* <https://us.sunpower.com/sites/default/files/sp-gen2-solar-cell-ds-en-a4-160-506760e.pdf>

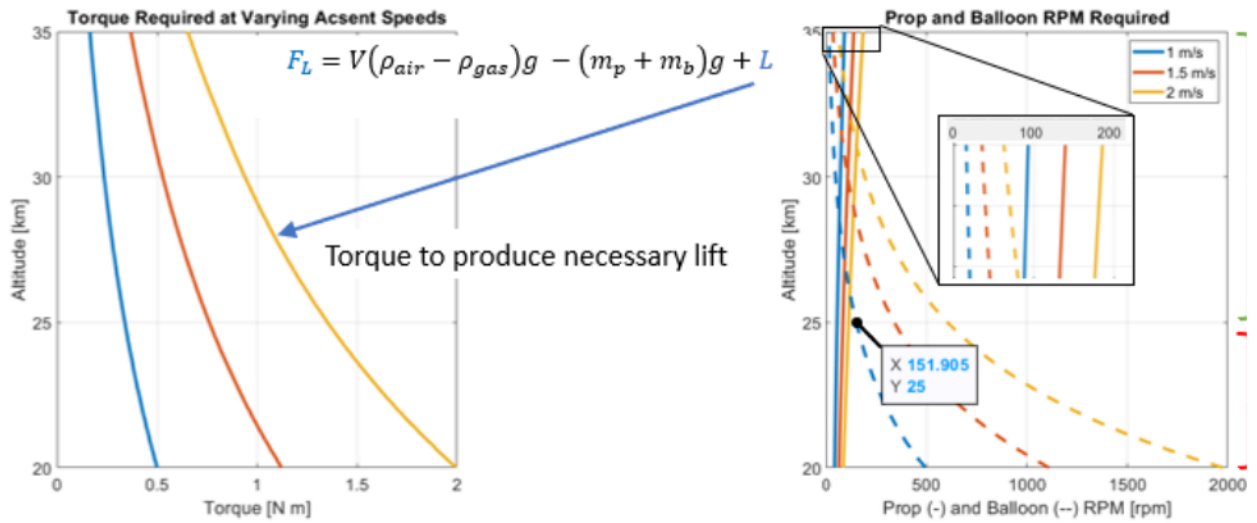


**Fig. 9.** Left: Torque requirements for the motor spinning the gossamer blades as a result of atmospheric drag acting on the blade surface at differing translation speeds from 1-2 m/s. Right: Blade (solid) and balloon (dashed) RPM at differing translation speeds. Note the balloon RPM is much larger for most of the flight regime due to the reduction in balloon radius with which the viscous drag acts.

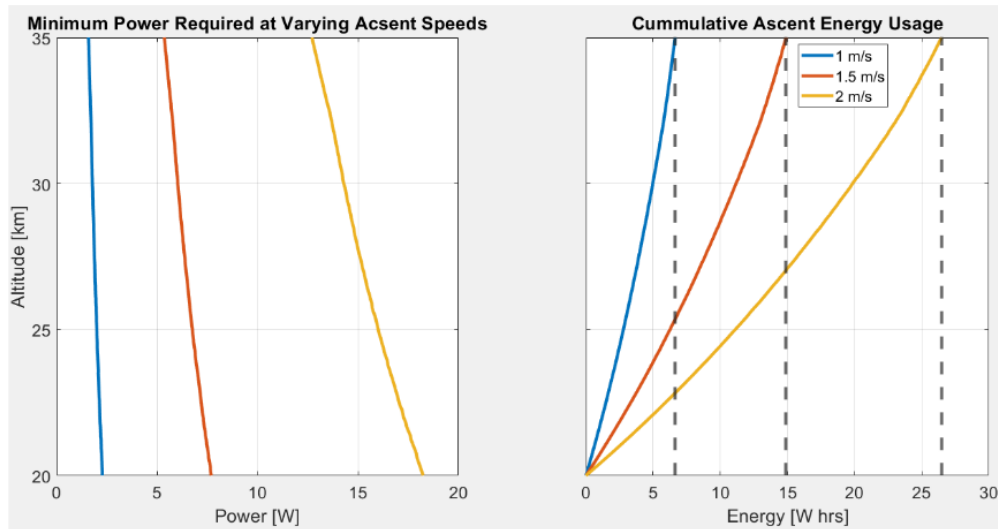


**Fig. 10.** Left: Idealized power requirements for a balloon translating at various speeds through the flight regime. Right: Cumulative energy consumed for a single translation from 20 - 35 km.

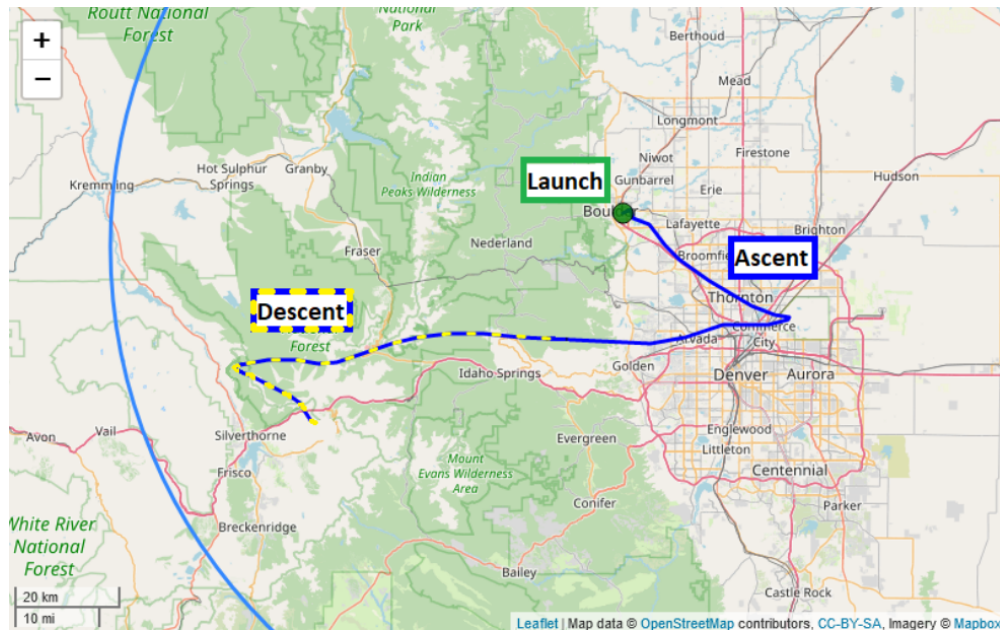


**Fig. 11.** Predicted natural balloon trajectory with venting at apogee (33 km) on July 31st, 2022 demonstrating eastern and western winds with a small northerly component, making station keeping without significant southern drift impossible.

## 4. Capabilities

While the capabilities of a lift augmented balloon are still being explored, a number of concepts appear possible. In addition to altitude profiling up and down, missions which require a consistent altitude hold could be enhanced with a lift augmentation device by enabling precise altitude maintenance for long (possibly indefinite) durations. Such a capability is not currently possible on small, inexpensive balloons.

Additionally, in some situations when wind shear layers meet mission requirements, altitude control can enable rudimentary station keeping, provided the mission allows for changes in altitude to do so. This concept was analyzed in (7), where it was demonstrated via simulation that given sufficiently varied wind layers, a balloon could remain over a point on the ground within a 25 km radius for several days. This is highly dependent on wind profiles however, and Fig. (11) shows an instance where a launch over Boulder, CO could enable East-West station keeping, but the balloon would consistently drift to the South since there is no altitude where a strong southerly wind exists.

Lift augmentation also lends itself well to exploration of other planets. Balloon missions to both Mars (15), (16) and Venus (9), (17) have been proposed or conducted (18). With weight being such a critical constraint for spaceflight, the possibility of using smaller, lightweight balloons for future planetary exploration could be attractive. Unlike some of the other methods described which require complex pumping systems or specific choices of lifting gas, the principles of lift augmentation are widely applicable to other atmospheres. The upper flight levels of the HYFLITS campaign are already operating in similar conditions to those on Mars, as seen in Fig. (12), with weather soundings of National Weather Service launches

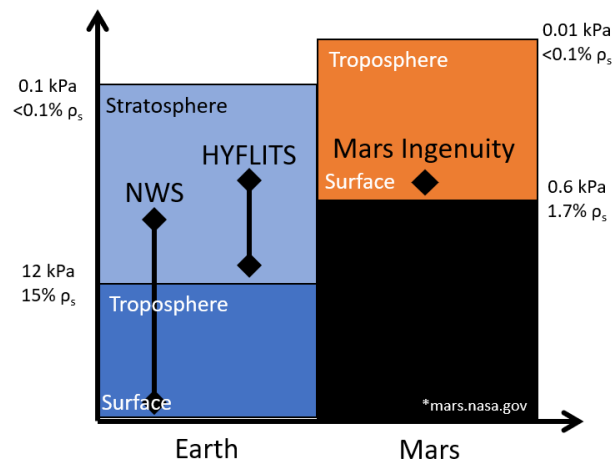


**Fig. 12.** Atmospheric pressure and density across typical flight regimes for National Weather Service and HYFLITS balloon launches compared to the on Mars.

also shown for scale.

Future work will go towards further characterizing the effectiveness of lift augmentation on different mission concepts.

## 5. Conclusion

Lift augmentation of balloons using gossamer blades presents a new possible solution to the problem of balloon control, particularly for smaller, lower-cost balloon campaigns. Some questions still remain, namely what kinds of missions could be enabled or enhanced with lift augmentation, the scalability of the concept to other balloons or environments, and a more thorough examination of the stability of the blades as they undergo changes in the blade angle of attack.

The existing prototype, in conjunction with the feasibility model and existing blade stability models, are well outfitted to address these questions. Model updates are planned to be made over the coming year. These results can be tested directly on the Ver. 4 testing rig with minimal modification, allowing for rapid verification. Following that, full scale flight tests could be conducted to further validate the concept for application to new mission proposals.

## References

- 1 Andrey Sushko, Aria Tedjarati, Joan Creus-Costa, Sasha Maldonado, Kai Marshland, and Marco Pavone. Low cost, high endurance, altitude-controlled latex balloon for near-space research (ValBal). In *2017 IEEE Aerospace Conference*, pages 1–9, March 2017. .
- 2 Christopher A. Roseman, Dale A. Lawrence, Joseph L. Pointer, Steve Borenstein, and Brian M. Argrow. A Low-Cost Balloon System for High-Cadence, In-Situ Stratospheric Turbulence Measurements. In *AIAA AVIATION 2021 FORUM*, AIAA AVIATION Forum. American Institute of Aeronautics and Astronautics, July 2021. . URL <https://arc.aiaa.org/doi/10.2514/6.2021-2691>.
- 3 Andreas Kräuchi, Rolf Philipona, Gonzague Romanens, Dale F. Hurst, Emrys G. Hall, and Allen F. Jordan. Controlled weather balloon ascents and descents for atmospheric research and climate monitoring. *Atmospheric Measurement Techniques*, 9(3):929–938, March 2016. ISSN 1867-1381. . URL <https://amt.copernicus.org/articles/9/929/2016/>. Publisher: Copernicus GmbH.
- 4 Paul B. Voss, Emily E. Riddle, and Michael S. Smith. Altitude Control of Long-Duration Balloons. *Journal of Aircraft*, 42(2):478–482, March 2005. ISSN 0021-8669, 1533-3868. . URL <https://arc.aiaa.org/doi/10.2514/1.7481>.
- 5 N. Yajima, N. Izutsu, and H. Honda. Structure variations of pumpkin balloon. *Advances in Space Research*, 33(10):1694–1699, January 2004. ISSN 0273-1177. . URL <https://www.sciencedirect.com/science/article/pii/S0273117703011463>.
- 6 Sherif Saleh and Weiliang He. New design simulation for a high-altitude dual-balloon system to extend lifetime and improve floating performance. *Chinese Journal of Aeronautics*, 31(5):1109–1118, May 2018. ISSN 1000-9361. . URL <https://www.sciencedirect.com/science/article/pii/S1000936118301018>.
- 7 Huafei Du, Mingyun Lv, Jun Li, Weiyu Zhu, Lanchuan Zhang, and Yifei Wu. Station-keeping performance analysis for high altitude balloon with altitude control system. *Aerospace Science and Technology*, 92:644–652, September 2019. ISSN 1270-9638. . URL <https://www.sciencedirect.com/science/article/pii/S1270963819312271>.
- 8 K Nock, K Aaron, J Jones, D McGee, G Powell, A Yavrouian, and J Wu. Balloon ALtitude Control Experiment (ALICE) project. In *11th Lighter-than-Air Systems Technology Conference*, Lighter-Than-Air Conferences. American Institute of Aeronautics and Astronautics, May 1995. . URL <https://arc.aiaa.org/doi/10.2514/6.1995-1632>.
- 9 Geoffrey Landis. Low-Altitude Exploration of the Venus Atmosphere by Balloon. In *48th AIAA Aerospace Sciences Meeting Including the New Horizons Forum and Aerospace Exposition*, Aerospace Sciences Meetings. American Institute of Aeronautics and Astronautics, January 2010. . URL <https://arc.aiaa.org/doi/10.2514/6.2010-628>.
- 10 David Cease, Nolan Ferguson, Braden Barkmeyer, Ryan Lansdon, Kelly Crombie, Jacob Marvin, Jared Dempewolf, Kyle McGue, Tyler Faragallah, and Paolo Wilczak. High Altitude Lifting Orbiter (HALO) Project Final Report. page 94, May 2020. URL [https://www.colorado.edu/aerospace/sites/default/files/attached-files/halo\\_pfr.pdf](https://www.colorado.edu/aerospace/sites/default/files/attached-files/halo_pfr.pdf).
- 11 Bob Balam, Timothy Canham, Courtney Duncan, Håvard F. Grip, Wayne Johnson, Justin Maki, Amelia Quon, Ryan Stern, and David Zhu. Mars Helicopter Technology Demonstrator. In *2018 AIAA Atmospheric Flight Mechanics Conference*, AIAA SciTech Forum. American Institute of Aeronautics and Astronautics, January 2018. . URL <https://arc.aiaa.org/doi/10.2514/6.2018-0023>.
- 12 W. Keats Wilkie, Jerry E. Warren, Daniel V. Guerrant, Dale A. Lawrence, S. Chad Gibbs, Earl H. Dowell, Andrew F. Heaton, Andrew F. Heaton, Jer-Nan Juang, Lucas G. Horta, Karen H. Lyle, Justin D. Littell, Robert G. Bryant, Mark W. Thomson, and Phillip E. Walkemeyer. Heliogyro Solar Sail Research at NASA. Glasgow, June 2013. URL <https://ntrs.nasa.gov/citations/20130014933>. NTRS Author Affiliations: NASA Langley Research Center, Colorado Univ., Duke Univ., NASA Marshall Space Flight Center, Jet Propulsion Lab., California Inst. of Tech. NTRS Report/Patent Number: NF1676L-16171 NTRS Document ID: 20130014933 NTRS Research Center: Langley Research Center (LaRC).
- 13 A. Gallice, F. G. Wienhold, C. R. Hoyle, F. Immler, and T. Peter. Modeling the ascent of sounding balloons: derivation of the vertical air motion. *Atmospheric Measurement Techniques*, 4(10):2235–2253, October 2011. ISSN 1867-1381. . URL <https://amt.copernicus.org/articles/4/2235/2011/>. Publisher: Copernicus GmbH.
- 14 U. Lei, C. Y. Yang, and K. C. Wu. Viscous torque on a sphere under arbitrary rotation. *Applied Physics Letters*, 89(18):181908, October 2006. ISSN 0003-6951. . URL <https://aip.scitation.org/doi/10.1063/1.2372704>. Publisher: American Institute of Physics.
- 15 V. V. Kerzhanovich, J. A. Cutts, H. W. Cooper, J. L. Hall, B. A. McDonald, M. T. Pauken, C. V. White, A. H. Yavrouian, A. Castano, H. M. Cathey, D. A. Fairbrother, I. S. Smith, C. M. Shreves, T. Lachenmeier, E. Rainwater, and M. Smith. Breakthrough in Mars balloon technology. *Advances in Space Research*, 33(10):1836–1841, January 2004. ISSN 0273-1177. . URL <https://www.sciencedirect.com/science/article/pii/S0273117703011682>.
- 16 Terry Gamber, Kerry Nock, J. Balam, Matthew Heun, I. Smith, Kerry Nock, J. Balam, Matthew Heun, I. Smith, and Terry Gamber. Mars 2001 Aerobot/Balloon System overview. In *International Balloon Technology Conference*, Balloon Systems Conferences. American Institute of Aeronautics and Astronautics, June 1997. . URL <https://arc.aiaa.org/doi/10.2514/6.1997-1447>.
- 17 E. Chassefière, O. Korablev, T. Imamura, K. H. Baines, C. F. Wilson, D. V. Titov, K. L. Aplin, T. Balint, J. E. Blamont, C. G. Cochran, Cs. Ferencz, F. Ferri, M. Gerasimov, J. J. Leitner, J. Lopez-Moreno, B. Marty, M. Martynov, S. V. Pogrebenko, A. Rodin, J. A. Whiteway, and L. V. Zasova. European Venus Explorer: An in-situ mission to Venus using a balloon platform. *Advances in Space Research*, 44(1):106–115, July 2009. ISSN 0273-1177. . URL <https://www.sciencedirect.com/science/article/pii/S0273117709000672>.

- 18 R. Z. Sagdeev, V. M. Linkin, J. E. Blamont, and R. A. Preston. The VEGA Venus Balloon Experiment. *Science*, 231(4744): 1407–1408, March 1986. . URL <https://www.science.org/doi/abs/10.1126/science.231.4744.1407>. Publisher: American Association for the Advancement of Science.